Diffusion and Viscoelasticity of Copolymer Micelles in a Homopolymer Matrix

Hiroshi Watanabe,* Tomohiro Sato, and Kunihiro Osaki

Institute for Chemical Research Kyoto University, Uji, Kyoto 611-0011 Japan

Mark W. Hamersky,[†,‡] Bryan R. Chapman,[‡] and Timothy P. Lodge*[,§]

Department of Chemical Engineering and Materials Science and Department of Chemistry, University of Minnesota, Minneapolis, Minnesota 55455-0431

Received January 26, 1998

Revised Manuscript Received April 3, 1998

Introduction

Watanabe, Osaki, and co-workers have recently reported detailed linear and nonlinear viscoelastic measurements on poly(styrene-*b*-isoprene) (SI) spherical micelles dispersed in nonentangling polyisoprene (I) matrices.[1−4] Measurements were conducted at temperatures below the glass transition of the styrene cores so that the micelles were effectively internally crosslinked. As the concentration of micelles was increased, a transition from liquidlike to solidlike behavior was clearly evident. For the liquidlike solutions, three relaxation processes were well resolved in the (linear) dynamic shear modulus G^*. The fastest corresponded to the relaxation of the unentangled matrix homopolymer. The intermediate mode was assigned to the relaxation spectrum of the corona isoprene blocks, based on favorable comparison with the terminal relaxation behavior of polyisoprene stars.[1−3] The slowest mode was tentatively attributed to micellar diffusion, an interpretation supported by estimates of the diffusivity using the Stokes−Einstein relation, and on the similarity of both the linear[1,3] and nonlinear[2−4] viscoelastic responses to that reported for suspensions of silica spheres.[5−7] For suspensions of hard spheres, this terminal relaxation is understood as the diffusive recovery to an isotropic spatial distribution of particles.[5,8−13] However, to assess this assignment, we have undertaken direct measurements of the micellar diffusion coefficients by forced Rayleigh scattering.

Experimental Section

Materials. The styrene−isoprene block copolymer, designated SI(14-29) and isoprene homopolymer, designated I-4, were synthesized by anionic polymerization as previously described.[1] The molecular weights are 13 900 and 28 800 for the styrene and isoprene blocks, respectively, and 4100 for the polyisoprene; polydispersities are less than 1.06 for the copolymer and 1.05 for the homopolymer. A portion of the copolymer was labeled at the styrene block end with azobenzene for the FRS measurements, by termination with 4-(phenylazo)benzoyl chloride.[1]

Rheology. Linear viscoelastic measurements were performed on blends containing 8, 15, 20, 25, and 30% SI(14-29) by weight, using a Rheometrics RDA II, as previously described.[1] Blends with $c_{SI} \leq 20\%$ clearly exhibited the terminal flow behavior characteristic of random dispersions of micelles, whereas those with $c_{SI} = 25$ and 30% showed a low-frequency plateau in the elastic modulus, G', indicative of a micellar lattice. The short I-4 matrix polymer swells the corona isoprene blocks but does not entangle with them. In addition there are no intermicellar entanglements for $c_{SI} = 8$ and 15%, whereas intermicellar entanglements begin to contribute to the moduli for $c_{SI} \geq 20\%$.[1] FRS measurements were performed for the three lower concentrations, $c_{SI} = 8$, 15, and 20%.

Forced Rayleigh Scattering. Samples were prepared by codissolving appropriate amounts of labeled and unlabeled SI(14-29) and I-4 in benzene, filtering through an 0.45 μm filter, and removing the solvent by slow evaporation followed by drying under vacuum to constant weight. Each sample was then transferred to an optical cell consisting of two glass disks separated by a 1 mm thick spacer ring, which was finally sealed under argon. The concentration of labeled chains was maintained at 8−10% in the three blends.

FRS measurements were made in the phase-grating mode at 30.0 °C.[14,15] Transient grating signals were recorded at three to five different grating spacings, d, over a range from 1 to 5 μm. This length scale is about 2 orders of magnitude greater than the micellar dimensions, and thus a long-time diffuson coefficient can be determined. As reported in previous FRS investigations of diblock micellar diffusion under "wet brush" conditions,[16] the relaxation kinetics exhibited two modes that were well-separated in time and made comparable contributions to the total diffracted intensity. The slower mode, which determines the long-time relaxational behavior, was consistently well-described by a single-exponential function

$$I(t) = (A_s \exp(-t/\tau_s) + C_1)^2 + C_2^2 \quad (1)$$

where A_s is the fraction of the diffracted field amplitude associated with the slow mode, τ_s is the corresponding relaxation time, and C_1 and C_2 represent coherent and incoherent background scattering contributions, respectively. A typical example is shown in Figure 1. The diffusion coefficient for this mode was determined from a plot of $1/\tau_s$ vs $1/d^2$ (found to be linear in all cases), according to

$$\frac{1}{\tau_s} = \frac{4\pi^2 D}{d^2} + \frac{1}{\tau_o} \quad (2)$$

where τ_o is the thermal lifetime of the cis isomer of the azobenzene moiety.

In contast to the slow mode, the fast mode could not be accurately described by a single-exponential function, suggesting the presence of a distribution of relaxation times. It was possible to fit the entire decay using a stretched exponential for the faster portion, i.e.

$$I(t) = (A_f \exp[-(t/\tau_f)^\beta] + A_s \exp(-t/\tau_s) + C_1)^2 + C_2^2 \quad (3)$$

where the subscript f denotes the faster mode parameters; a fit utilizing eq 3 is also shown in Figure 1. With decreasing d the values of β decreased from ca. 0.5 to 0.1 and the quality of the overall fit deteriorated noticeably. Consequently, we cannot provide a definitive analysis of this mode at this point. This faster relaxation possibly reflects nondiffusive motions of the micelles, (i.e., caging effects, rotation) and/or contributions from free chain diffusion, as suggested by Schaertl et al.[17]

Results and Discussion

In the previous work the reduced modulus of the micelles, $G^*_{SI,r}(\omega)$, was determined as

* Authors for correspondence.

[†] Department of Chemical Engineering and Materials Science, University of Minnesota.

[‡] Current address: The Procter & Gamble Company, Miami Valley Laboratories, Cincinnati, OH 45247.

[§] Department of Chemistry, University of Minnesota.

S0024-9297(98)00100-4 CCC: $15.00
Published on Web 05/08/1998

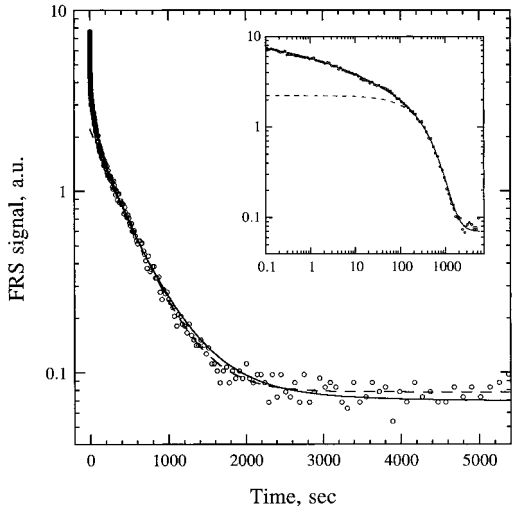

Figure 1. Typical FRS decay for $c_{SI} = 20\%$ at 30 °C with $d = 3.14\ \mu$m. Key: dashed line, fit to eq 1 ($\tau_s = 790$ s); solid line, fit to eq 3 ($\tau_f = 15.3$ s, $\beta = 0.25$, $\tau_s = 816$ s). The inset shows the same data in double logarithmic format.

$$G^*_{SI,r}(\omega) \equiv \left(\frac{M_{bI}}{c_{bI}RT}\right)(G^*_{blend}(\omega) - \phi_{I-4}G^*_{I-4}(\omega)) \quad (4)$$

where c_{bI} and M_{bI} are the concentration and molecular weight of the corona isoprene blocks, and the subtracted term on the rhs represents the matrix ("solvent") contribution.[1] At the frequencies of interest here, this term was much smaller than $G^*_{blend}(\omega)$ and thus represents a minor correction. The elastic and loss contributions to $G^*_{SI,r}(\omega)$ are shown in Figure 2. Two modes are evident, with the faster occurring at frequencies $\omega a_T > 10^3$ rad/s. The slower mode has a much stronger dependence on c_{SI}.

As mentioned in the Introduction, the faster mode was previously assigned to the relaxation of the corona blocks, which is expected to be similar to the relaxation of the arm of a star.[1,18] Thus, in Figure 2 the smooth curves represent the reduced modulus for a star, $G^*_{star,r}(\omega)$, defined as

$$G^*_{star,r}(\omega) \equiv \left(\frac{M_{arm}}{\rho RT}\right)G^*_{star}(\omega) \quad (5)$$

where the $G^*_{star}(\omega)$ data were obtained in the melt for a four-arm polyisoprene star with $M_{arm} = 36\,700$,[19] which is similar to M_{bI}. For comparison to the SI/I blends with different concentrations, the star data are plotted against $\omega(\tau_{star}/\tau_{f,VE})$, where $\tau_{f,VE}$ is the viscoelastic relaxation time for the faster process (determined previously[1]) and τ_{star} is the terminal time for the star melt. In Figure 2 it is apparent that the fast relaxation process for the micelles and the terminal relaxation process for the stars are in good accord, supporting the assigment of the former to orientational relaxation of the tethered corona blocks.[1,3]

We take advantage of this coincidence to use the $G^*_{star,r}$ data (plotted against $\omega(\tau_{star}/\tau_{f,VE})$) as a reduced modulus for the fast process of the micelles, to extract the terminal relaxation time for the slow micellar process, $\tau_{1,VE}$, as follows. At sufficiently low ω, both $G^*_{fast,r}$ ($=G^*_{star,r}$) and $G^*_{SI,r}$ ($=G^*_{fast,r} + G^*_{slow,r}$) exhibit terminal behavior: $G' = G\omega^2 \sim \omega^2$ and $G'' = \eta\omega \sim \omega$, with G and η representing elasticity and viscosity coefficients, respectively; see Figure 2. Thus we determined these coefficients in the respective terminal regimes (e.g., $\omega a_T < 10^3$ s^{-1} for $G^*_{fast,r}$ and $\omega a_T < 30$ s^{-1} for $G^*_{SI,r}$, both for $c_{SI} = 8\%$) to evaluate the viscoelastic relaxation time as

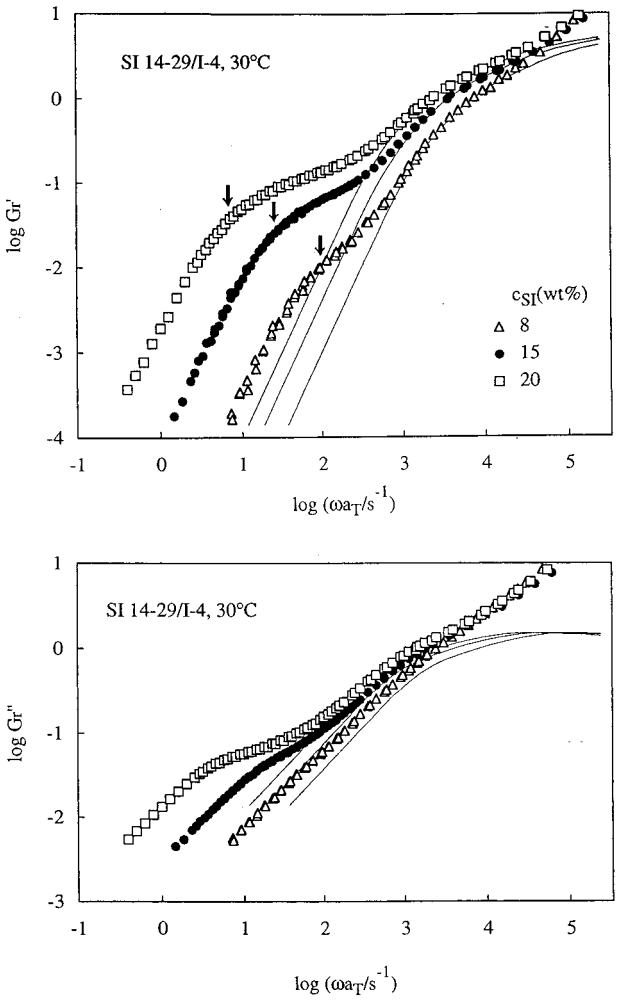

Figure 2. Reduced dynamic shear moduli for blends of SI-(14-19) in I-4. The smooth curves correspond to data for polyisoprene stars, as discussed in the text. The arrows denote the (inverse) longest relaxation times for the micelles determined from eq 6.

Table 1

c_{SI}/wt %	$\log(\tau_{1,VE}/s)$	$\log(D/cm^2s^{-1})$	δ/Å
8	−1.99	−10.59	126
15	−1.41	−11.07	141
20	−0.84	−11.70	132

$$\tau_{1,VE} \equiv \frac{G_{SI} - G_{fast}}{\eta_{SI} - \eta_{fast}} = \frac{\int_{-\infty}^{\infty} H_{slow}(\tau)\tau^2\ d(\ln \tau)}{\int_{-\infty}^{\infty} H_{slow}(\tau)\tau\ d(\ln \tau)} \quad (6)$$

This $\tau_{1,VE}$, related to the relaxation spectrum H_{slow} of the slow process as indicated above, is close to the longest viscoelastic relaxation time of the SI micelles, as shown by the thick arrows in Figure 2 (the definition of $\tau_{1,VE}$ differs slightly from that utilized previously,[1] i.e., $\tau_{s,VE} = G_{SI}/\eta_{SI}$).

These longest relaxation times and the diffusion coefficients associated with the slow FRS mode, both obtained at 30 °C with estimated uncertainties better than ±30%, are collected in Table 1. An average distance, δ, that an SI micelle diffuses during an

interval $\tau_{1,VE}$, is obtained as

$$\delta \equiv (6D\tau_{1,VE})^{1/2} \quad (7)$$

The values of δ are also collected in Table 1. Even though both D and $\tau_{1,VE}$ change by more than an order of magnitude over this concentration range, δ is effectively constant, at 133 ± 10 Å. Interestingly, this distance corresponds closely to the estimated diameter of the styrene micellar cores, 160 Å.[1] Thus we may conclude that the terminal relaxation process of the micelles corresponds to the diffusion of the micelles over a distance of approximately one micellar core.

For highly concentrated spherical silica particles, the longest viscoelastic relaxation time corresponds to diffusion over distances comparable to the particle diameter, but the diffusion coefficient in question is the short-time diffusion coefficient,[5] in contrast to the long-time or tracer diffusion coefficient measured here by FRS. For the relatively dilute SI micelles examined here, any difference between the short-time and long-time diffusion coefficients could be rather small. Thus it remains an interesting unresolved question whether the terminal relaxation of heavily interentangled micelles will still correspond to the tracer diffusion coefficient over the same distance scale.

Acknowledgment. Ths work was supported in part by the National Science Foundation, through Award DRM-9528481 (T.P.L.), and by the Center for Interfacial Engineering, an NSF-supported Engineering Research Center at the University of Minnesota.

References and Notes

(1) Sato, T.; Watanabe, H.; Osaki, K.; Yao, M.-L. *Macromolecules* **1996**, *29*, 3881.
(2) Watanabe, H.; Sato, T.; Osaki, K.; Yao, M.-L. *Macromolecules* **1996**, *29*, 3890.
(3) Watanabe, H. *Acta Polym.* **1997**, *48*, 215.
(4) Watanabe, H.; Yao, M.-L.; Sato, T.; Osaki, K. *Macromolecules* **1997**, *30*, 5905.
(5) Shikata, T.; Pearson, D. S. *J. Rheol.* **1994**, *38*, 601.
(6) Watanabe, H.; Yao, M.-L.; Yamagishi, A.; Osaki, K.; Shikata, T.; Niwa, H.; Morishima, Y. *Rheol. Acta* **1996**, *35*, 433.
(7) Watanabe, H.; Yao, M.-L.; Osaki, K.; Shikata, T.; Niwa, H.; Morishima, Y. *Rheol. Acta* **1997**, *36*, 524.
(8) Bender, J. W.; Wagner, N. J. *J. Colloid Interface Sci.* **1995**, *172*, 171.
(9) Bender, J. W.; Wagner, N. J. *J. Rheol.* **1996**, *40*, 899.
(10) Bossis, G.; Brady, J. F. *J. Chem. Phys.* **1989**, *91*, 1866.
(11) Brady, J. F. *J. Chem. Phys.* **1993**, *99*, 567.
(12) Wagner, N. J.; Ackerson, B. J. *J. Chem. Phys.* **1992**, *97*, 1473.
(13) Mackay, M. E.; Kaffashi, B. *J. Colloid Interface Sci.* **1995**, *174*, 117.
(14) Huang, W. J.; Frick, T. S.; Landry, M. R.; Lee, J. A.; Lodge, T. P.; Tirrell, M. *AIChE J.* **1987**, *33*, 573.
(15) Lodge, T. P.; Chapman, B. R. *Trends Polym. Sci.* **1997**, *5* 122.
(16) Inoue, T.; Nemoto, N.; Kurata, M. *Bull. Inst. Chem. Res. Kyoto Univ.* **1988**, *66*, 194.
(17) Schaertl, W.; Tsutsumi, K.; Kishishima, K.; Hashimoto, T. *Macromolecules* **1996**, *29*, 5297.
(18) Raju, V. R.; Menezes, E. V.; Marin, G.; Graessley, W. W.; Fetters, L. J. *Macromolecules* **1981**, *14*, 1668.
(19) Fetters, L. J.; Kiss, A. D.; Pearson, D. S.; Quack, G. F.; Vitus, F. J. *Macromolecules* **1993**, *26*, 647.

MA980100D